nature medicine

Silencing mutant SOD1 using RNAi protects against neurodegeneration and extends survival in an ALS model

G Scott Ralph[1], Pippa A Radcliffe[1], Denise M Day[1], Janine M Carthy[1], Marie A Leroux[1], Debbie C P Lee[1], Liang-Fong Wong[1], Lynsey G Bilsland[2], Linda Greensmith[2], Susan M Kingsman[1], Kyriacos A Mitrophanous[1], Nicholas D Mazarakis[1] & Mimoun Azzouz[1]

Amyotrophic lateral sclerosis (ALS) is a fatal neurodegenerative disease resulting in the selective death of motor neurons in the brain and spinal cord[1]. Some familial cases of ALS are caused by dominant mutations in the gene encoding superoxide dismutase (*SOD1*)[2–4]. The emergence of interfering RNA (RNAi) for specific gene silencing could be therapeutically beneficial for the treatment of such dominantly inherited diseases[5–7]. We generated a lentiviral vector to mediate expression of RNAi molecules specifically targeting the human *SOD1* gene (*SOD1*). Injection of this vector into various muscle groups of mice engineered to overexpress a mutated form of human *SOD1* (*SOD1*^{G93A}) resulted in an efficient and specific reduction of *SOD1* expression and improved survival of vulnerable motor neurons in the brainstem and spinal cord. Furthermore, *SOD1* silencing mediated an improved motor performance in these animals, resulting in a considerable delay in the onset of ALS symptoms by more than 100% and an extension in survival by nearly 80% of their normal life span. These data are the first to show a substantial extension of survival in an animal model of a fatal, dominantly inherited neurodegenerative condition using RNAi and provide the highest therapeutic efficacy observed in this field to date.

RNAi has become established as a powerful tool for highly specific gene silencing, and viral vectors delivering short hairpin RNAs (shRNAs) have been shown to be effective in the central nervous system (CNS)[8,9]. An efficient RNAi-based strategy for treating *SOD1*-linked ALS would require delivery of the therapeutic molecule to susceptible motor neuron populations. Lentiviral vectors based on the equine infectious anemia virus (EIAV) provide ideal candidate vehicles for such delivery, as they have proven particularly efficient at targeting motor neurons of the spinal cord and brainstem through retrograde transport after intramuscular injection[10–12]. Several lines of transgenic mice expressing mutated forms of human *SOD1* develop a form of motor neuron disease that closely resembles clinical and pathological phenotypes of ALS[4,13,14]. Here we investigated the potential of EIAV vectors to induce silencing of mutant *SOD1* expression in the *SOD1*^{G93A} transgenic mouse, a widely used animal model of ALS[4,12,15].

We identified putative RNAi target sites for *SOD1* silencing using online algorithms. The two sequences containing the least sequence homology to mouse *Sod1* were chosen for evaluation. We generated EIAV vectors to express these target sequences as shRNA molecules downstream from *RPPH1* (encoding ribonuclease P RNA component H1) promoter[16] (EIAV-SOD1HP1, EIAV-SOD1HP2; **Fig. 1a**). Control vectors were also constructed to mediate expression of a shRNA targeted against the gene encoding firefly luciferase[16] (EIAV-LucHP) and an empty expression cassette (EIAV-Emp). We assessed the efficiency of EIAV-mediated *SOD1* silencing by transducing each vector into a human cell line. Transduction with either control vector had no effect on *SOD1* expression compared with untransduced controls 7 d after transduction, both at the level of protein and mRNA expression (**Fig. 1b**,**c**). Transduction with the vector EIAV-SOD1HP1, however, resulted in a significant reduction in *SOD1* mRNA compared with control-transduced samples ($P < 0.05$, $n = 3$) and a similar decrease in protein expression. Transduction of EIAV-SOD1HP2 resulted in a smaller and insignificant decrease in *SOD1* mRNA but showed no detectable differences in SOD1 protein levels. The expression of functional shRNAs from EIAV-LucHP was confirmed by the reduction of luciferase protein levels in cells that were cotransduced with a vector overexpressing the reporter gene encoding firefly luciferase (EIAV-Luciferase; **Fig. 1b**). From these results we can confirm that the reduction in *SOD1* expression by EIAV-SOD1HP1 was specific and not caused by a nonspecific effect mediated by general expression of shRNA molecules.

To determine the efficacy of EIAV-SOD1HP1–mediated silencing of *SOD1* expression in primary neuronal cells, we transduced cortical neurons derived from *SOD1*^{G93A} embryos with EIAV vectors. High transduction efficiencies were achieved, with ~95% of neurons staining positive for LacZ, the reporter gene encoding β-galactosidase (**Fig. 1d**). Analysis of *SOD1* expression showed a reduction in protein levels at day 4 (50%) and day 7 (70%) and a highly significant decrease in *SOD1* mRNA ($P < 0.005$, $n = 5$) at day 7 after transduction with EIAV-SOD1HP1 compared with controls (**Fig. 1e**,**f**). We also observed

[1]Oxford Biomedica (UK) Ltd, Medawar Centre, The Oxford Science Park, Oxford, OX4 4GA, UK. [2]Sobell Department of Motor Neuroscience and Movement Disorders, Institute of Neurology, Queen Square, London, WC1N 3BG, UK. Correspondence should be addressed to G.S.R. (s.ralph@oxfordbiomedica.co.uk) or M.A. (m.azzouz@oxfordbiomedica.co.uk).

Published online 13 March 2005; doi:10.1038/nm1205

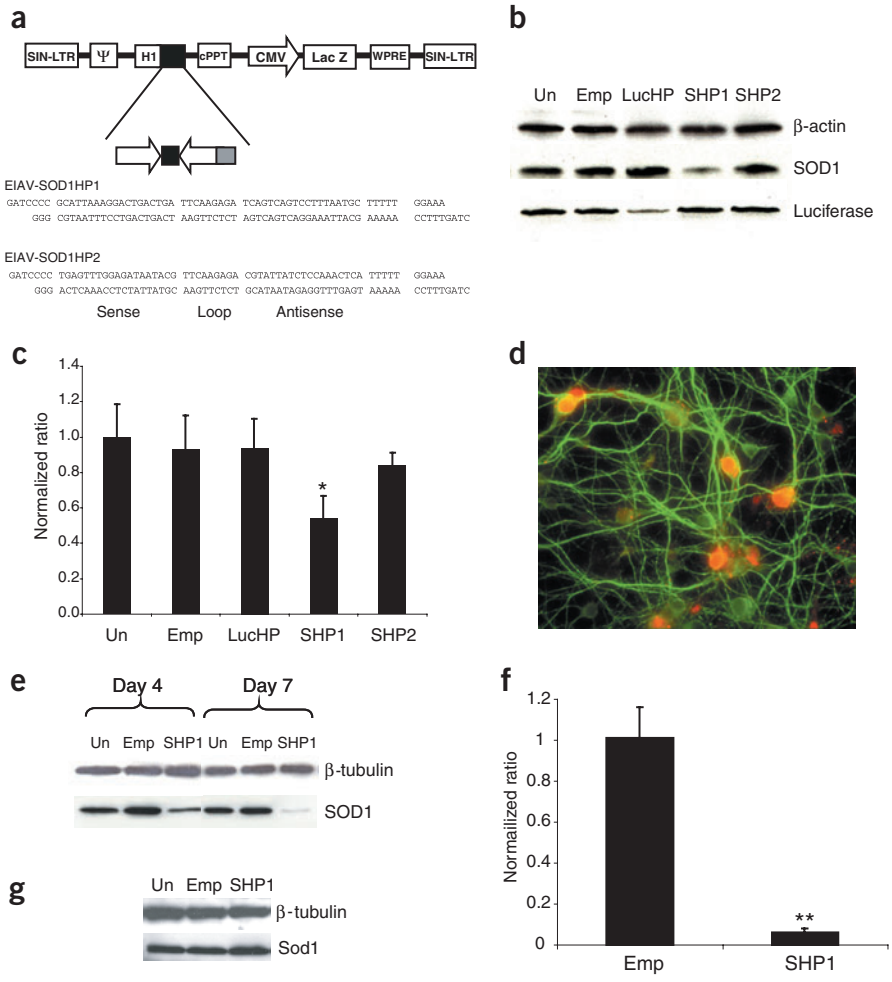

Figure 1 Silencing of *SOD1* expression *in vitro* using EIAV-mediated expression of shRNAs. (**a**) EIAV genome encoding *SOD1* shRNA target sequences as shown. Analysis of (**b**) human SOD1 and firefly luciferase protein and (**c**) *SOD1* mRNA in HEK293T cells 7 d after transduction. (**d**) Immunofluorescence analysis of EIAV-SOD1HP1–mediated β-galactosidase expression (red) and microtubule associated protein-2 (green) in primary cortical neurons derived from $SOD1^{G93A}$ mice. Analysis of (**e**) SOD1 protein expression 4 and 7 d after transduction and (**f**) *SOD1* mRNA levels at 7 d after transduction of $SOD1^{G93A}$ primary cortical neurons. (**g**) Analysis of mouse Sod1 protein expression in transduced cortical neurons from wild type mice. $^{*}P < 0.05$, $n = 3$; $^{**}P < 0.005$, $n = 5$, two-tailed Student *t*-test. SIN-LTR, self-inactivating long terminal repeat; Ψ, EIAV packaging signal; CMV, cytomegalovirus promoter; Un, untreated; Emp, EIAV-Emp treated; SHP1, EIAV-SOD1HP1 treated; SHP2, EIAV-SOD1HP2 treated.

silencing of *SOD1* expression in primary astrocyte and mixed ventral horn cultures from $SOD1^{G93A}$ mice transduced with EIAV-SOD1HP1 (data not shown). Analysis of wild-type mouse Sod1 protein showed no reduction in expression, indicating that the silencing effects of shRNA delivery were specific for the human *SOD1* (**Fig. 1g**). This is a particularly important observation for *in vivo* studies because this eliminates the possibility of nonspecific effects from targeting wild-type expression.

We generated rabies-G–pseudotyped EIAV vectors to evaluate the efficacy of *SOD1* silencing *in vivo*. The high transduction efficiency (>50%) of spinal motor neurons in the ventral horn of the lumbar spinal cord after injection of EIAV vectors into the hindlimb muscles (**Fig. 2a**,**b**) was similar to that previously reported[12]. Furthermore, analysis of SOD1 expression showed a 40% reduction of protein levels in ventral horn tissue of mice, 2 weeks after injection with EIAV-SOD1HP1 into hindlimb muscles (**Fig. 2c**).

To investigate the potential therapeutic effects of silencing mutant *SOD1* expression, we injected $SOD1^{G93A}$ mice intramuscularly with EIAV vectors at 7 d of age. The muscle groups injected were specifically chosen because they are critical for mobility (hindlimb), respiration (diaphragm and intercostal) and feeding (facial and tongue), and thus are essential for determining general health and survival of these mice. To analyze motor function, we subjected animals to the well-established rotarod test[12,17–19]. Animals were monitored for disease onset (**Fig. 2d**) as defined by a reduction in rotarod performance and end stage of disease (**Fig. 2e**). Mice injected with EIAV-Emp showed an onset of motor impairment at 94 d of age (**Fig. 2d** and **3a**). This was not significantly different from uninjected $SOD1^{G93A}$ control mice (EIAV-Emp, 94.1 ± 5.0 d, $n = 7$; untreated, 94.3 ± 2.9 d, $n = 5$). After onset of ALS symptoms, all control mice deteriorated progressively, showing a lack of mobility, failure to groom their fur, hindlimb dysfunction, breathing difficulties and signs of muscle atrophy. In contrast, EIAV-SOD1HP1–injected animals showed a highly significant delay in the onset of any motor symptoms compared with controls (202.1 ± 7.5 d; $P < 0.001$, $n = 6$), representing an increase in the age of onset by 115% (**Fig. 2d** and **3a**). Furthermore, following the late onset of rotarod deficits in these animals, we also observed differences in disease progression, with mice developing a general weakness and immobility, but not showing severe signs of hindlimb dysfunction, even at the end stage of disease. These observations imply that motor neuron innervation of the hindlimbs was at least partially maintained in these animals.

Mice were killed at the end stage of disease, which was defined as the time at which the animals were unable to right themselves within 30 s of being placed on their sides. Mice injected with EIAV-Emp ($n = 7$) or untreated controls ($n = 5$) survived for a mean of 129.3 ± 1.6 d and 128.3 ± 2.9 d, respectively (**Fig. 2e**). This represents a typical life span of $SOD1^{G93A}$ mice[4]. Survival of EIAV-SOD1HP1–injected animals was significantly extended compared to controls, with a mean life span of 227.8 ± 11.3 d ($P < 0.001$, $n = 6$). This represents an increase in survival by 77%. Analysis of transgene copy number confirmed that the effects on survival observed were not a consequence of a reduced copy number of the $SOD1^{G93A}$ transgene in EIAV-SOD1HP1–injected mice (**Supplementary Fig. 1** online).

To further quantify neuromuscular performance of $SOD1^{G93A}$ mice during this study, we performed footprint analysis of hindlimb stride length (**Fig. 3b**). This analysis showed significant impairment in the walking patterns of EIAV-Emp–injected mice at 90 and 120 d of age compared with EIAV-SOD1HP1 animals ($P < 0.01$ and $P < 0.005$, respectively, $n = 6$). No significant differences, however,

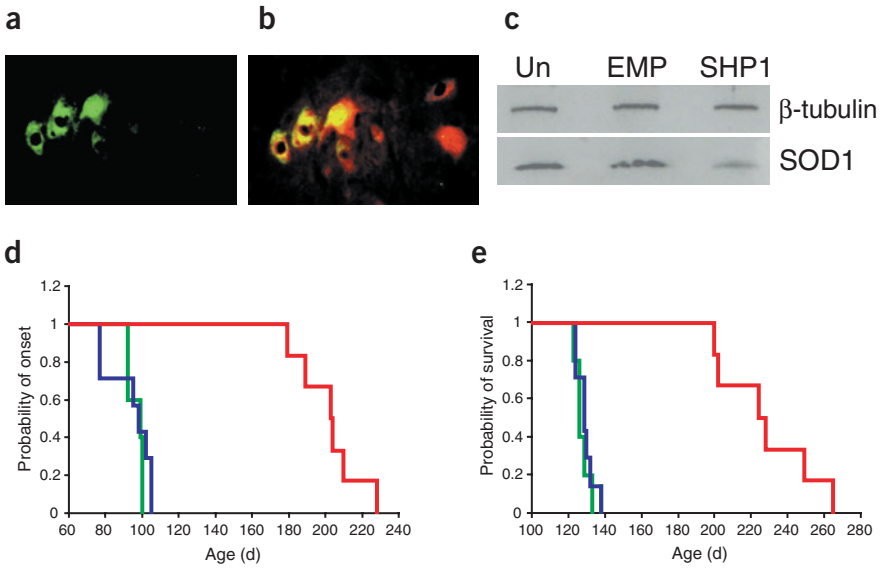

Figure 2 Silencing of mutant *SOD1* expression *in vivo* delays onset of ALS and extends survival of *SOD1*^{G93A} mice. Immunofluorescence of (**a**) β-galactosidase (green) and (**b**) calcitonin gene-related peptide (red) in spinal cord sections from *SOD1*^{G93A} mice after intramuscular injection of EIAV-SOD1HP1 into hindlimb muscles. (**c**) Western blot analysis of EIAV-SOD1HP1–mediated silencing of SOD1 protein in the ventral horn of the lumbar spinal cord. (**d**) Onset of ALS symptoms and (**e**) survival analysis of *SOD1*^{G93A} mice injected at 7 d of age with EIAV vectors. Data represents EIAV-SOD1HP1-injected (red; $n = 6$), EIAV-Emp–injected (blue; $n = 7$) and uninjected (green; $n = 5$) *SOD1*^{G93A} mice.

were observed in EIAV-SOD1HP1–injected mice compared with wild-type mice up to 180 d of age (**Fig. 3b**). Analysis of animal weight showed that weight gain in control-injected mice was halted at the time of disease onset (94 d) and mice declined in weight thereafter (**Fig. 3c**). Mice injected with EIAV-SOD1HP1 had significantly higher body weights than controls ($P < 0.05$, $n = 6$) and weight loss was not observed until 160 d of age.

Histological analysis of spinal cord and brain stem sections taken from control-injected *SOD1*^{G93A} mice at the end stage of disease showed typical ALS neuropathology, with severe motor neuron death and vacuole formation (**Fig. 4a**,**c**). Conversely, sections taken from EIAV-SOD1HP1 animals showed an increase in the survival of motor neurons in both the spinal cord and facial nucleus (**Fig. 4b**,**d**), indicating that the populations of motor neurons targeted by EIAV expression of shRNA were protected from degeneration. Counts of surviving ventral horn motor neurons confirmed significant protection of these cells from degeneration compared with controls ($P < 0.005$, $n = 3$; **Fig. 4e**). These findings imply that death of EIAV-SOD1HP1–injected mice was not necessarily a consequence of motor neuron degeneration, and this correlates well with the altered disease progression. We also observed positive β-galactosidase expression in surviving spinal cord motor neurons from EIAV-SOD1HP1–injected animals that was not present in degenerating neurons (**Fig. 4f**). This result confirms long-term expression from EIAV vectors and shows the protective effect of EIAV-SOD1HP1 on transduced motor neurons.

In summary, we have shown that EIAV-mediated silencing of mutant *SOD1* expression in vulnerable motor neuron populations using shRNA causes long-term reversal of a dominantly inherited form of ALS in a transgenic mouse model. Previous gene therapy approaches for ALS have involved the delivery of neurotrophic factors to susceptible cells[12,20]. Efficacy in those studies, however, has been limited to an extension in the life expectancy of transgenic mice by approximately 30%[12,20]. The improved survival observed here is probably a consequence of the direct approach used for targeting the genetic factor underlying the disease. Expression of mutant *SOD1* in non-neuronal cells has some role in causing motor neuron degeneration in ALS[21] and increased efficacy may be further achieved by silencing mutant *SOD1* expression in such cell types. Nonetheless, the noninvasive mode of vector delivery used in this study and the substantial efficacy achieved shows the enormous and realistic potential for advancing vector-based RNAi approaches to the clinic. Indeed, this vector system is already under clinical development for therapeutic delivery of the angiogenic factor vascular endothelial growth factor to treat ALS[12].

These studies highlight the considerable therapeutic potential of RNAi for treating dominantly inherited disease and provide optimism for the future progression of RNAi from a research tool to a therapeutic agent.

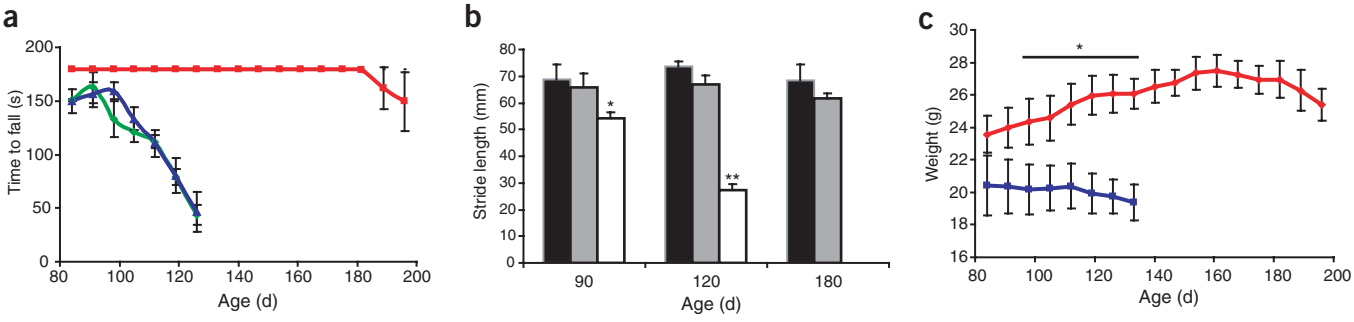

Figure 3 Silencing of *SOD1* expression using shRNA mediates improved motor performance in *SOD1*^{G93A} transgenic mice. (**a**) Rotarod performance in transgenic mice injected with EIAV-SOD1HP1 (red, $n = 6$), EIAV-Emp (blue, $n = 7$) and uninjected controls (green, $n = 5$). (**b**) Hindlimb footprint analysis of stride length in EIAV-SOD1HP1–injected (gray), EIAV-Emp–injected (white) and wild-type (black) mice showing a significant improvement in stride length by shRNA expression compared with injected controls (*$P < 0.01$, **$P < 0.005$, $n = 4$). (**c**) Weight measurements of EIAV-SOD1HP1–injected (red) and EIAV-Emp–injected (blue) animals. Mice receiving intramuscular injection of EIAV-SOD1HP1 were significantly heavier than injected controls (*$P < 0.05$, $n = 6$).

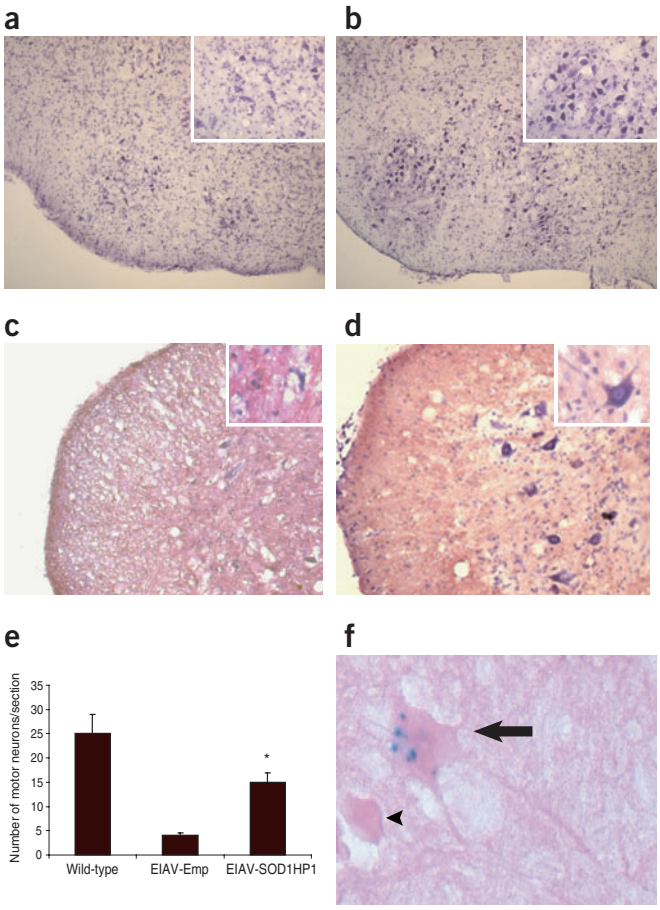

Figure 4 Motor neuron survival is improved by RNAi-mediated silencing of *SOD1*. Cresyl violet staining of facial nucleus (**a**,**b**) and lumbar spinal cord sections (**c**,**d**) from EIAV-injected mice at the end stage of disease (low magnification, ×10; high magnification, ×40). Survival of motor neurons was higher in EIAV-SOD1HP1–injected mice (**b**,**d**) compared with control-injected animals (**a**,**c**). (**e**) Quantification of surviving spinal motor neurons at the end stage of disease. (**f**) Long-term expression of β-galactosidase in spinal motor neurons of EIAV-SOD1HP1–treated mice at the end stage of disease. EIAV-SOD1HP1 transduction (blue staining) protects against neuronal degeneration (arrow). Arrowhead indicates degenerating untransduced cell. $^*P < 0.005$, $n = 3$.

METHODS

Construction of EIAV Vectors. We amplified the *RPPH1* promoter from genomic DNA extracted from the human embryonic kidney 293T (HEK293T) cell line using the following primers: (forward) 5′-AATATGCTGCAGGAATTC GAACGCTGACGTCAT-3′ and (reverse) 3′-AGCATAGCTCAGCTGCAGCCTA GGTGCATAAGATCTGTGGTCTCATACAGA-3′ and cloned it into the *PstI* site of the vector EIAV-NCZ. Putative short interfering RNA target sequences were designed against the human *SOD1* gene using online algorithms (Dharmacon). Sequences were determined to be unique to the human *SOD1* gene by BLAST searching of GenBank database. Oligonucleotide primers were designed corresponding to the sense and antisense sequences of the siRNA target sites of interest separated by a hairpin loop sequence[16]. We annealed primers and cloned them into EIAV-NCZH1 downstream of the *RPPH1* promoter (**Fig. 1**).

Viral vector production. We prepared EIAV vector stocks pseudotyped with the vesicular stomatitis virus-G envelope protein (VSV-G) or the rabies wild-type envelope protein (ERA-WT) by transient transfection of the HEK 293T cell line as previously described[22,23]. Viral titers were in the range of 7×10^8–1×10^9 transducing units/ml. These were estimated using quantitative RT-PCR by comparison with the vector pONY8.0GFP[10] and normalized for viral RNA[24].

Animal model. We used transgenic mice carrying the human *SOD1* gene with the G93A mutation in these studies[4]. The mouse line was maintained as a hemizygote by breeding G93A males with C57B16/SJL hybrid females. Transgenic progeny were identified by PCR using primers specific for human *SOD1* (ref. 4). We confirmed the genotype of the mice used for these studies two more times by this method during the course of the experiment, including at the late stage of disease. To eliminate the possibility of increased survival being a consequence of a dropped copy number of the $SOD1^{G93A}$ gene, littermates of EIAV-SOD1HP1–injected animals were used as either injected or noninjected controls in these experiments. Furthermore, transgene copy number was confirmed by quantitative RT-PCR as described below. Animals were housed in a standard environment of 12-h light–12-h dark cycle. We carried out all animal procedures with permission from and according to the United Kingdom Home Office Regulations.

Vector delivery. Rabies-G–pseudotyped EIAV vectors were injected intramuscularly into 7 d old $SOD1^{G93A}$ transgenic mice. We injected each mouse with a total of 120 μl viral vector into the following muscle groups: hindlimb (60 μl), facial (20 μl), tongue (10 μl), diaphragm (15 μl) and intercostals (15 μl). Multiple sites of injections were used for each muscle group, with a total of 5 μl vector injected per site.

Cell culture. We maintained HEK293 cells under standard conditions in Dulbecco Modified Eagle Medium (Sigma) supplemented with 2 mM L-glutamine (Sigma) and 10% fetal calf serum (Sigma). Primary cortical neurons were prepared from E-18 mouse embryos. Cortices from individual embryos were dissected and maintained separately in Hank balanced salt solution (Invitrogen). We digested tissue with papain (1 mg/ml) for 15 min at 37 °C and dissociated it using a plastic pipette. Cells were plated at a density of 2×10^5 cells per well in a 12-well plate previously coated with poly-D-lysine (5 μg/ml). Cultures were maintained in Neurobasal media (Invitrogen) supplemented with 1% B27 (Invitrogen) and 1 mM L-glutamine. For all *in vitro* experiments, we transduced cells withVSV-G-pseudotyped EIAV vectors using a multiplicity of infection of 10 transducing units/cell.

Quantitative RT-PCR. To analyze *SOD1* mRNA levels, we extracted RNA from cells (RNeasy kits, Qiagen) and used it as a template for cDNA synthesis using oligo (dT) primers with the Superscript II cDNA synthesis kit (Roche Diagnostics). Real-time quantitative PCR was performed using the ABI Prism 7700 detection system with a SYBR green DNA detection kit (Applera). Expression levels of the housekeeping gene encoding β-actin were also quantified and used for normalization. To confirm that the transgene copy number of $SOD1^{G93A}$ was not altered in the mice used for this study, we evaluated genomic *SOD1* levels by RT-PCR using genomic DNA isolated from tail tissue. We estimated transgene copy number by comparing values with a standard curve of known *SOD1* copy numbers using human genomic DNA. Analysis of the mouse housekeeping gene encoding glyceraldehyde-3-phosphate dehydrogenase was used for normalization purposes. All primers were designed using Primer Express 2.0 (Applera) and used at a concentration of 300 nM. Standard cycling conditions were used.

Western blotting. Protein samples were extracted from cultured cells using cell lysis buffer (Tropix). For analysis of *SOD1* expression *in vivo*, the ventral horn region of the lumbar spinal cord was microdissected from the entire cord and homogenized in lysis buffer (Promega). Equal amounts of protein (15 μg) were fractionated by SDS-PAGE. Following transfer onto a nitrocellulose membrane (Amersham Biosciences) blots were probed with an antibody to human SOD1 (1:1,000, Chemicon), a rabbit polyclonal antibody to SOD1 (1:1,000, Santa Cruz Biotechnology), a mouse monoclonal antibody to firefly luciferase (1:1,000, Merck), a mouse monoclonal antibody to β-tubulin (1:1,000, Chemicon) or a polyclonal antibody to β-actin (1:1,000, Sigma) followed by the relevant horseradish peroxidase–conjugated immunoglobulin (Dako). We developed blots using ECL reagent (Amersham Biosciences) and quantified band area using Image J Software (US National Institutes of Health).

Behavioral analysis. Mice were assessed for motor dysfunction using the rotarod task every 7 d from 70 d of age onward. Briefly, we placed animals on an accelerating rod (Economex Rotarod, Columbus Instruments) and recorded the time it took for each mouse to fall from the rod. We performed three trials at each time point for each animal and recorded the longest time taken to fall and used it in analyses. A cut-off time point was set at 180 s and mice remaining on the rod for at least this period of time were deemed asymptomatic[12,17–19]. Onset of disease symptoms was determined as a reduction in rotarod performance between weekly time points.

Footprint analyses were performed by placing the hind feet of mice into ink and recording walking patterns during continuous locomotion. We measured stride length as the distance between prints and an average of three stride lengths taken for each animal at each time point evaluated.

Cell counts. All cell counts were performed in a blinded fashion. In brief, we counted the numbers of transduced cells in every fifth section throughout the entire lumbar spinal cord. Only the large-size neurons with a clear nucleolus and distinctly labeled cytoplasm were included in cell counts. We performed counts at a magnification of ×40. The coefficient of error was determined as described previously[25].

Statistical analysis. Statistical significance was assessed using a Student paired *t*-test or analysis of variance (ANOVA) as stated in the figure legends.

Note: Supplementary information is available on the Nature Medicine website.

ACKNOWLEDGMENTS

Many thanks to the Virology and Neurobiology teams at Oxford BioMedica for assistance with design and preparation of viral vectors. L.G.B. is a Wellcome Trust Prize student. L.G. is the Graham Watts Senior Research Fellow funded by the Brain Research Trust. This work was funded by Oxford Biomedica Ltd.

COMPETING INTERESTS STATEMENT

The authors declare competing financial interests (see the *Nature Medicine* website for details).

Received 31 August 2004; accepted 17 February 2005
Published online at http://www.nature.com/naturemedicine/

1. Mulder, D.W. Clinical limits of amyotrophic lateral sclerosis. *Adv. Neurol.* **36**, 15–22 (1982).
2. Rosen, D.R. *et al.* Mutations in Cu/Zn superoxide dismutase gene are associated with familial amyotrophic lateral sclerosis. *Nature* **362**, 59–62 (1993).
3. Deng, H.X. *et al.* Amyotrophic lateral sclerosis and structural defects in Cu,Zn superoxide dismutase. *Science* **261**, 1047–1051 (1993).
4. Gurney, M.E. *et al.* Motor neuron degeneration in mice that express a human Cu,Zn superoxide dismutase mutation. *Science* **264**, 1772–1775 (1994).
5. Maxwell, M.M., Pasinelli, P., Kazantsev, A.G. & Brown, R.H., Jr. RNA interference-mediated silencing of mutant superoxide dismutase rescues cyclosporin A-induced death in cultured neuroblastoma cells. *Proc. Natl. Acad. Sci. USA* **101**, 3178–3183 (2004).
6. Ding, H. *et al.* Selective silencing by RNAi of a dominant allele that causes amyotrophic lateral sclerosis. *Aging Cell* **2**, 209–217 (2003).
7. Xia, H. *et al.* RNAi suppresses polyglutamine-induced neurodegeneration in a model of spinocerebellar ataxia. *Nat. Med.* **8**, 816–820 (2004).
8. Xia, H., Mao, Q., Paulson, H.L. & Davidson, B.L. siRNA-mediated gene silencing *in vitro* and *in vivo*. *Nat. Biotechnol.* **20**, 1006–1010 (2002).
9. Hommel, J.D., Sears, R.M., Georgescu, D., Simmons, D.L. & DiLeone, R.J. Local gene knockdown in the brain using viral-mediated RNA interference. *Nat. Med.* **9**, 1539–1544 (2003).
10. Mazarakis, N.D. *et al.* Rabies virus glycoprotein pseudotyping of lentiviral vectors enables retrograde axonal transport and access to the nervous system after peripheral delivery. *Hum. Mol. Genet.* **10**, 2109–2121 (2001).
11. Wong, L.F. *et al.* Transduction patterns of pseudotyped lentiviral vectors in the nervous system. *Mol. Ther.* **9**, 101–111 (2004).
12. Azzouz, M. *et al.* VEGF delivery with retrogradely transported lentivector prolongs survival in a mouse ALS model. *Nature* **429**, 413–417 (2004).
13. Wong, P.C. *et al.* An adverse property of a familial ALS-linked SOD1 mutation causes motor neuron disease characterized by vacuolar degeneration of mitochondria. *Neuron* **14**, 1105–1116 (1995).
14. Bruijn, L.I. *et al.* ALS-linked SOD1 mutant G85R mediates damage to astrocytes and promotes rapidly progressive disease with SOD1-containing inclusions. *Neuron* **18**, 327–338 (1997).
15. Cleveland, D.W. & Rothstein, J.D. From Charcot to Lou Gehrig: deciphering selective motor neuron death in ALS. *Nat. Rev. Neurosci.* **2**, 806–819 (2001).
16. Brummelkamp, T.R., Bernards, R. & Agami, R.A system for stable expression of short interfering RNAs in mammalian cells. *Science* **296**, 550–553 (2002).
17. Katsuno, M. *et al.* Testosterone reduction prevents phenotypic expression in a transgenic mouse model of spinal and bulbar muscular atrophy. *Neuron* **35**, 843–854 (2002).
18. Katsuno, M. *et al.* Leuprorelin rescues polyglutamine-dependent phenotypes in a transgenic mouse model of spinal and bulbar muscular atrophy. *Nat. Med.* **9**, 768–773 (2003).
19. Adachi, H. *et al.* Transgenic mice with an expanded CAG repeat controlled by the human AR promoter show polyglutamine nuclear inclusions and neuronal dysfunction without neuronal cell death. *Hum Mol. Genet.* **10**, 1039–1048 (2001).
20. Kaspar, B.K., Llado, J., Sherkat, N., Rothstein, J.D. & Gage, F.H. Retrograde viral delivery of IGF-1 prolongs survival in a mouse ALS model. *Science* **301**, 839–842 (2003).
21. Clement, A.M. *et al.* Wild-type nonneuronal cells extend survival of SOD1 mutant motor neurons in ALS mice. *Science* **302**, 113–117 (2003).
22. Mitrophanous, K. *et al.* Stable gene transfer to the nervous system using a non-primate lentiviral vector. *Gene Ther.* **6**, 1808–1818 (1999).
23. Soneoka, Y. *et al.* A transient three-plasmid expression system for the production of high titer retroviral vectors. *Nucleic Acids Res.* **23**, 628–633 (1995).
24. Martin-Rendon, E., White, L.J., Olsen, A., Mitrophanous, K.A. & Mazarakis, N.D. New Methods to Titrate EIAV-Based Lentiviral Vectors. *Mol. Ther.* **5**, 566–570 (2002).
25. Abercrombie, M. Estimation of nuclear population from microtome sections. *Anatomical Record* **94**, 239–247 (1948).